Charge Inversion of Mono- and Di-anions to Cations via Triply Charged Metal Complexes: Application to Lipid Mixtures

Kimberly C. Fabijanczuk, David J. Foreman, and Scott A. McLuckey*

Department of Chemistry

Purdue University

West Lafayette, IN, 47907-2084, USA

*Address correspondence to:
Dr. Scott A. McLuckey
560 Oval Drive
Department of Chemistry
Purdue University
West Lafayette, IN 47907-2084, USA
Phone: (765) 494-5270
Fax: (765) 494-0239
E-mail: mcluckey@purdue.edu

Abstract

Electrospray ionization (ESI) of mixtures can give rise to ions with different masses and charges with overlapping mass-to-charge (*m/z*) ratios. Such a scenario can be particularly problematic for the detection of low-abundance species in the presence of more highly abundant mixture components. For example, negative mode ESI of polar lipid extracts can result in highly abundant singly-charged glyerophospholipids (GPLs), such as phosphatidylethanolamines (PE) and phosphatidylglycerols (PG), that can obscure much less abundant cardiolipins (CLs), which are complex phospholipids with masses roughly double those of GPLs that mostly form doubly-charged anions. Despite their low relative abundance, CLs are lipidome components that perform vital biological functions. To facilitate the study of CLs in lipid mixtures without resort to off-line or on-line separations, we have developed a gas-phase approach employing ion/ion reactions to charge invert anionic lipid species using a trivalent metal-complex. Specifically, ytterbium(III) is shown to readily complex with three neutral ligands, N,N,N',N'-tetra-2-ethylhexyl diglycolamide (TEHDGA), to form $[Yb(TEHDGA_3)]^{3+}$ using ESI. Herein, we describe pilot studies to evaluate $[Yb(TEHDGA)_3]^{3+}$ as an ion/ion reagent to allow for chemical separation of doubly- and singly-charge anions, using lipid mixtures as examples, without neutralizing ions of either charge state.

Introduction

Electrospray ionization (ESI) is a popular ionization technique in mass spectrometry (MS) for biomolecules such as peptides, proteins, lipids, etc.[1–3] ESI can generate various ion types such as protonated or metal-adducted species in positive ion mode, and deprotonated or anion-adducted species in negative ion mode. Furthermore, ESI has been shown to generate ion species with charges greater than one when multiple readily ionized sites are present.[1,4,5] The solution prior to being subjected to ESI can be manipulated to generate different ion-types, such as altering the pH or adding various salts.[6–9] This may be desirable to simplify mass spectra or change the ion-type to facilitate structural characterization via tandem MS.[10–12] However, modifying the solution to manipulate ion-type can suppress ion formation,[13] result in a more complicated mass spectrum, and/or result in the analyte no longer being in biologically relevant solvent conditions, as is the focus of 'native' mass spectrometry.[14] A straightforward alternative approach is to manipulate the ion-type post-ionization via gas-phase ion/ion reactions.[15–18] Gas-phase ion/ion reactions, when conducted within the context of a tandem MS experiment, allow for selective manipulation of ion-type by isolating a chosen reagent ion and then allowing it to react exclusively with a selected analyte ion. There are various ion transformation possibilities such as proton transfer,[15,19–21] metal transfer,[22–24] and covalent bond formation.[25–29]

We have previously reported using divalent alkaline earth metals complexed with tris 1,10-phenanthroline (phen)[30–33] and 2,2':6',2"-terpyridine (terpy)[34–37] to charge invert singly charged lipid species that allowed for in-depth structural characterization and isomeric differentiation. However, larger lipids such as Lipid A,[38] cardiolipin,[39] and phosphatidylinositol phosphate[40,41] preferentially ionize as dianions, precluding divalent metal complexes as suitable reagents for ion/ion reactions due to inevitable neutralization. Furthermore, all four major macromolecule classes (i.e., proteins, carbohydrates, oligonucleotides, and lipids) can give rise to anionic species with charges greater than one, especially larger and structurally complex species. Therefore, besides lipids, it would be beneficial to have more highly charged cationic reagents for ion-type manipulation for when a singly or doubly charged cation reagent does not improve analysis. Here, we extend our approach by introducing a novel cationic triply charged metal complex for charge inversion of lipid anions, specifically mono- and di-anions.

The lipidome constitutes a highly complex mixture and the informing power of mass spectrometry, by virtue of its sensitivity, selectivity, and speed, is a key tool in lipidomics.[42–44] Shot-gun lipidomics, in particular, has emerged as an attractive approach as there is minimal sample preparation and it avoids potentially long prior separations (e.g. liquid-chromatography-MS).[45,46] The lipidome in humans is incredibly complex and structurally diverse due to variations in head groups, number and length of fatty acyl chains, degree and location of unsaturation, and other modifications to the fatty acyl chains (e.g methyl, hydroxyl, or cyclopropyl groups).[43,47] While there has been much progress in the in-depth structural analysis and quantitation of lipids, there remain numerous challenges, such as localizing isomeric features including C=C position on the fatty acyl chains.[45,48]

Most shot-gun lipidomic experiments employ some form of ESI that is known to give rise to multiply charged species due to an analyte's structure, solution conditions, and/or spray conditions. This can complicate analysis when there are analyte ions of different mass and charge but similar mass-to-charge (m/z) ratios. This proves to be even more difficult when one analyte is significantly lower in abundance. There have been some approaches to address this issue from our group, such as gas-phase single proton transfer ion/ion reactions[32] and, most recently, a physical separation of lipid species within a mass spectrometer based on charge.[49] Single proton transfer can separate mono- and di-anions by converting the dianion to a monoanion while neutralizing the singly-charged anions. For example, we have previously employed gas-phase proton-transfer ion/ion reactions to transform cardiolipin (CL) dianions

from $[CL-2H]^{2-}$ to $[CL-H]^{1-}$ yielding a shift in *m/z* two times the original *m/z* making identification of cardiolipins straightforward.[32] Herein, we further expand the options for charge state manipulation by introducing a triply charged lanthanide-complex to charge-invert singly and doubly charged lipid anions to cations for identification and further analysis.

Experimental Section

Materials

All lipid standards: PE 16:0/18:1, CL 18:1/18:1 18:1/18:1, CL 16:0/18:1 16:0/18:1, Cardiolipin Mix 1, and *Escherichia coli* (*E. coli*) total lipid extract were purchased from Avanti Polar Lipids, Inc. (Alabaster, AL) and all used without further purification. Optima® LC/MS-grade methanol (MeOH), Optima® LC/MS-grade water (H_2O), Optima® acetonitrile (ACN), and HPLC-grade 2-Propanol were purchased from Fischer Scientific (Pittsburgh, PA). Ytterbium(III) nitrate pentahydrate ($Yb(NO_3)_3 \cdot 5H_2O$) was purchased from Sigma-Aldrich (St. Louis, MO). N,N,N',N'-tetra-2-ethylhexyl diglycolamide (TEHDGA) was purchased from AmBeed, Inc. (Arlington Heights, IL), catalog number: A766751.

Sample Preparation

PE 16:0/18:1, CL 18:1/18:1 18:1/18:1, and CL 16:0/18:1 16:0/18:1 was each dissolved separately into MeOH to a stock concentration of ~1mM. CL 16:0/18:1 16:0/18:1 was diluted further to 10 μM in MeOH. PE 16:0/18:1 and CL 18:1/18:1 18:1/18:1 was mixed to a final 1:1 molar ratio of 10 μM. *E. coli* lipid extract was dissolved into a stock solution of 1 mg/mL in MeOH and further diluted to a final concentration of 0.05 mg/mL in MeOH. $Yb(NO_3)_3 \cdot 5H_2O$ was dissolved in MeOH to an initial concentration of ~6 mM. TEHDGA was dissolved in 2-Propanol to an initial concentration of ~1 mM. TEHDGA at ambient temperature is viscous which can prove challenging to accurately measure so the calculated concentration may not be exact. $Yb(NO_3)_3 \cdot 5H_2O$ and TEHDGA were co-mixed to a final 1:1 molar ratio of 50 μM in MeOH with no further solution modifications.

Mass Spectrometry

All experiments were performed on a Sciex TripleTOF 5600 quadrupole time-of-flight mass spectrometer (SCIEX, Concord, ON, Canada) that has been previously modified for ion/ion reactions and dipolar DC (DDC).[50] Alternately pulsed nano-electrospray ionization (nESI) emitters allow for sequential injection of cations and anions.[51] Briefly, $[Yb(TEHDGA)_3]^{3+}$ was ionized via positive nESI, monoisotopically isolated in Q1, and transferred into the high-pressure collision cell, q2. Next, for lipid standards experiments, the standards were ionized via negative nESI, isolated in Q1, and transferred into q2 for mutual storage of 30 ms. When using *E. coli* lipid extract, the extract was ionized via negative nESI, transmitted through Q1 (no isolation) and into q2 for mutual storage of 30 ms. The resulting products from the ion/ion reaction were subsequently isolated and collisionally activated either using single frequency ion-trap collision induced dissociation (CID) or dipolar DC (DDC).[52] Mass analysis was performed via orthogonal acceleration time-of-flight measurements.

Results and Discussion

Selection of TEHDGA as ligand for trivalent metal complexes

In order to charge invert both singly- and doubly-charged anions, the reagent must be at least triply-charged. The necessary or desirable characteristics of a useful reagent ion for gas-phase reactions are:

i) inexpensive commercially available reagents, ii) minimal solution preparation requirements, iv) abundant and stable production of the target multiply charged species, and v) efficient execution of the desired chemistry. Based on our extensive experience in using doubly-charged complexes comprised of divalent metals with neutral ligands as charge inversion reagents for singly-charged lipid anions, we looked into the possibility for use of complexes of trivalent metals. We were unable to form strong signals for trivalent complexes using transition metal cations (e.g., Co^{3+}) with the ligands we often use for divalent metals (e.g., phen and terpy). We therefore explored the use of trivalent lanthanides with species commonly used for the extraction of lanthanides and actinides, such as the water soluble diglycolamides (DGAs).[53] Literature reports describe various DGAs used to stabilize tri and tetra-valent metals (e.g N,N,N',N'-tetramethyl-3-oxa-glutaramide (TMOGA)[54]), though most are not commercially available. TEHDGA is a commercially available DGA, which we found yields strong trivalent complexes when mixed with the commercially available $Yb(NO_3)_3 \cdot 5H_2O$ salt. (We did not do an exhaustive survey of trivalent lanthanides and actinides in combination with other candidate ligands due to the success with this combination of ligand and metal salt. We therefore anticipate that trivalent complexes comprised of other combinations of ligands and metals can also be generated efficiently using nESI.) **Figure 1A** demonstrates a positive nESI MS1 scan of the metal-ligand solution at a 1:1 molar ratio of 50μM, where L represents one TEHDGA ligand. There is evidence for protonated and sodiated ligand, $[L+H]^+$ (*m/z* 582) and $[L+Na]^+$ (*m/z* 603), as well as a sodium-bound dimer of the ligand, $[L_2+Na]^+$ (*m/z* 1184). There is evidence of doubly-charged species highlighted in pink that indicate the presence of Yb due to the isotopic distributions but were not further investigated as they were not the desired charge state. The base peak in the spectrum corresponds to $[Yb(L_3)]^{3+}$ (*m/z* 638), which is expanded in the inset to show the expected isotope distribution. It is noted that the isotopic abundances are undermeasured for the higher *m/z* isotopes which indicates a high mass discrimination that may due to the detection setup. The monoisotopic *m/z* of the complex, 638.5, has a calculated mass error of 1.903 ppm, which falls within instrument specifications. To avoid confusion in analysis, the triply charged metal complex'smost abundant isotope was isolated for all experiments besides the latter just discussed.

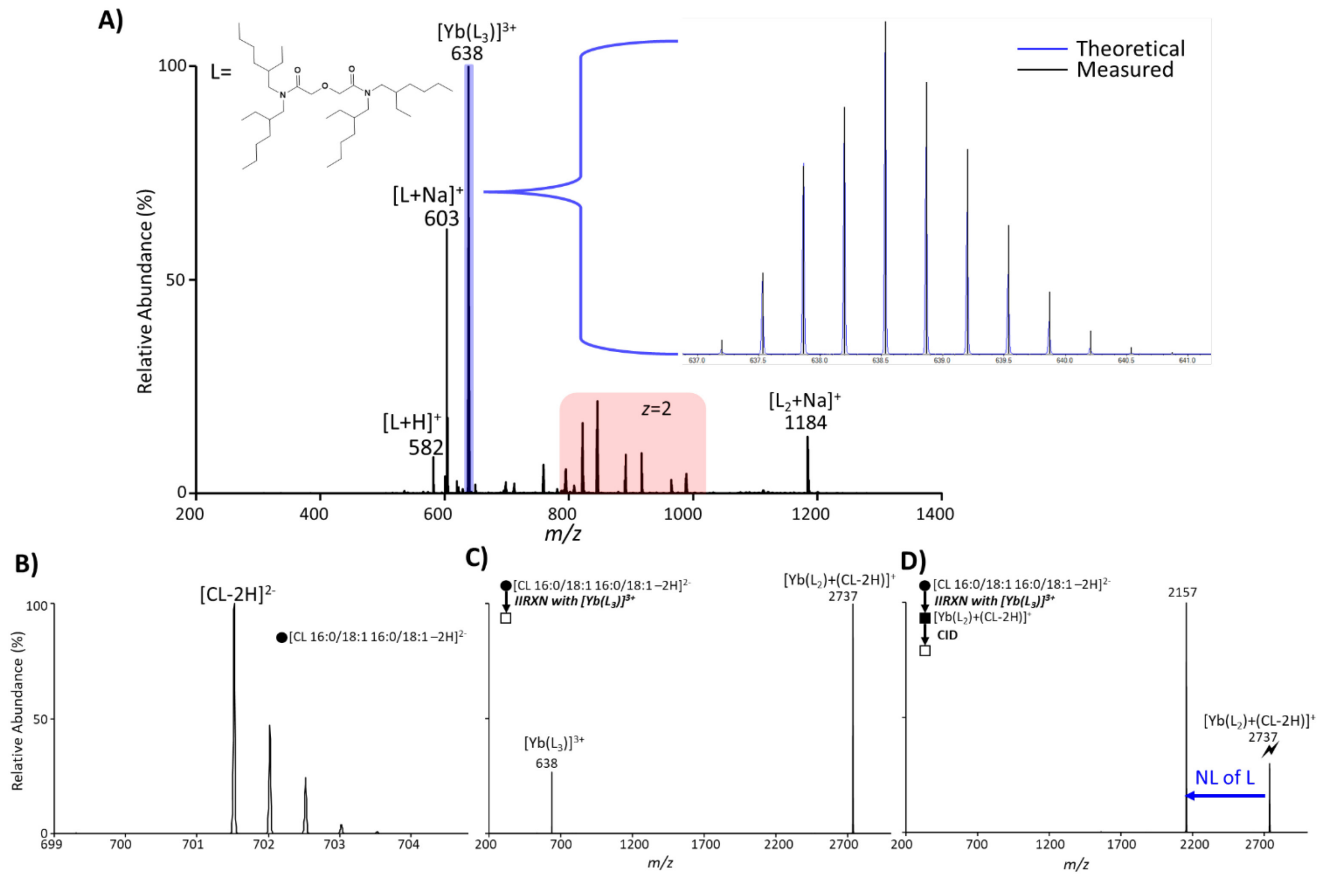

Figure 1. Ionization of $Yb^{III}(TEHDGA)_3$, gas-phase ion/ion reaction with a CL standard and $[Yb(TEHDGA)_3]^{3+}$, and subsequent collisional activation of the resulting complex. A) MS1 of positive nESI of 1:1 molar ratio 50μM of $Yb(NO_3)_3{\cdot}5H_2O$ and TEHDGA. The inset is a zoom in of $[Yb(TEHDGA)_3]^{3+}$overlayed with a theoretical isotope distribution. B) The negative mode spectrum of isolated [CL 16:0/18:1 16:0/18:1-2H]$^{2-}$. C) The resulting ion/ion reaction between $[Yb(TEHDGA)_3]^{3+}$ and [CL 16:0/18:1 16:0/18:1-2H]$^{2-}$. D) Subsequent CID of the resulting complex, $[Yb(L_2)+(CL-2H)]^+$.

Charge inversion of CL standards with $[Yb(TEHDGA)_3]^{3+}$

The ability of $[Yb(L_3)]^{3+}$ to charge invert dianion species was examined by considering the ion/ion reaction with [CL 16:0/18:1 16:0/18:1-2H]$^{2-}$ (*m/z* 701.5). To simplify the nomenclature, the fatty acyl information of the CL is removed from the label. **Figure 1B** displays the isolation of $[CL-2H]^{2-}$ generated by negative mode nESI. The triply charged-metal complex and CL dianion were mutually stored within a high-pressure (10 mtorr N_2) collision cell for ~30 ms and the resulting spectrum is shown in **Figure 1C**. Only one product ion is observed, a long-lived complex $[Yb(L_2)+(CL-2H)]^+$ (*m/z* 2737.3) that is formed via the union of the two reactants followed by neutral loss (NL) of one TEHDGA (580.6 Da). This demonstrates that a triply charged metal complex can efficiently charge invert a dianion in the gas-phase. The other ion observed in the spectrum is residual reagent, $[Yb(L_3)]^{3+}$, which can vary in abundance depending upon relative abundances of the reactants and the reaction time. CID of the resulting complex yielded a NL of another TEHDGA ligand to yield $[Yb(L)+(CL-2H)]^+$ (*m/z* 2156.7) shown in **Figure 1D**. This observation is reminiscent of our previous reports of using $Mg(phen)_3^{2+}$ dications to charge invert monoanion lipid species (e.g. unsaturated fatty acids) to cations via a complex formed by NL of one phen ligand and CID of the complex yielded another NL of one phen ligand.[30] CID after the second phen loss yielded structurally informative lipid fragments.

CID after the second TEHDGA loss from the complexes studied here also yields structurally informative fragment ions as shown in **Figure 2**. **Figure 2A** displays CID of the complex generated

from the first CID step (**Figure 1C**). The most abundant fragment ion at (*m/z* 1562.1) is assigned as cleavage of one of the phosphodiester linkages of the PA moieties resulting in the loss of glycerol-16:0/18:1. As both PA moieties are symmetrical, it is ambiguous as to whether the PA moiety at the 1' or 3' position of central glycerol backbone (or a mixture of the two) was lost. However, as shown below, for different FA sum composition for each PA moiety on a CL, there will be a pair of fragment ions representing each unique PA moiety. The other minor fragment ions observed are NL of the fatty acyl chains as acids, (*m/z* 1900.4) and (*m/z* 1874.4) for FA 16:0 and 18:1, respectively. Subsequent isolation and CID of $[Yb(L)+(CL\text{-}2H\text{-glycero }16:0/18:1)]^+$, shown in **Figure 2B** results in product ions (*m/z* 1323.8) from the NL of 16:0 as a ketene, (*m/z* 1305.8) from the NL of 16:0 as an acid, (*m/z* 1297.8) from the NL of 18:1 as a ketene, and (*m/z* 1279.8) from the NL of 18:1 as an acid. This fragmentation pattern allows for sum FA composition to be determined as well as individual FA identities (chain length and degree of unsaturation). The relative abundances for ions related to the loss of FA 16:0 in the *sn*-1 position are higher than those related to the loss of 18:1 in the *sn-2* position which supports previous reports that CLs with a 2- charge state favor *sn*-1 losses compared to *sn*-2 losses.[55]

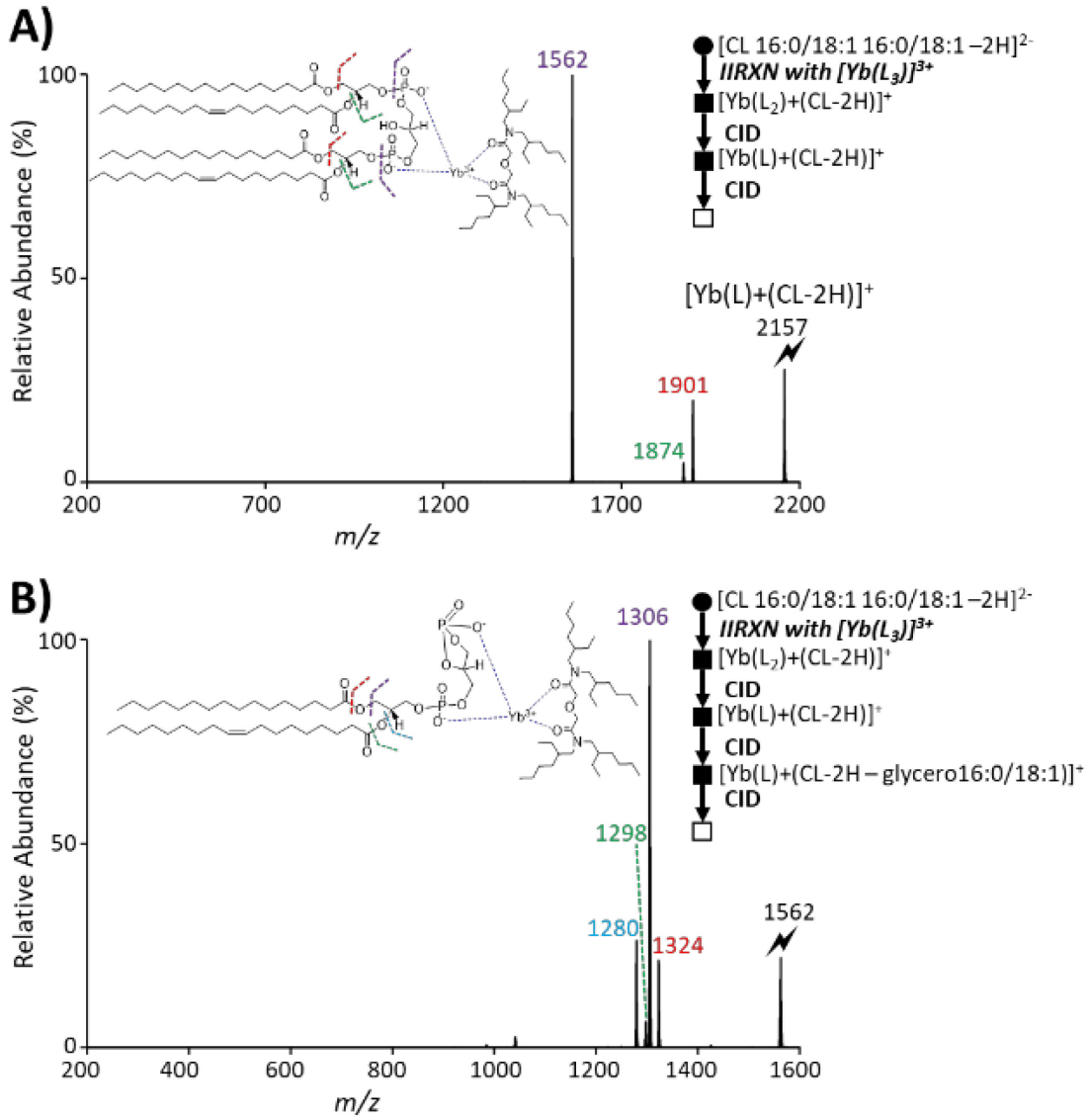

Figure 2. Tandem MS of the product ions following initial CID of, $[Yb(L_2)+(CL\text{-}2H)]^+$. A) CID of $[Yb(L)+(CL\text{-}2H)]^+$ (*m/z* 2157). B) CID of $[Yb(L)+(CL\text{-}2H\text{-glycero16:0/18:1})]^+$ (*m/z* 1562).

The ion/ion reaction phenomenology and results of the subsequent CID steps observed using CL 16:0/18:1 16:0/18:1, as illustrated in **Figures 1B** and **2**, appear to be universal for all CLs, which is supported by the data in **Figures 3**, **S1**, and **S2**. **Figure 3A** reflects the MS1 of nESI of Cardiolipin Mix 1 (see insert of **Figure 3A**) ionized in negative ion mode. The labels for each ion are color coded to reflect CL identity and the shaded boxes indicate ion-types with identical charges, which are listed in the adjacent box. The mix is reported by the vendor (Avanti Lipids) to consist of CL 14:1(3)-15:1, CL 15:0(3)-16:1, CL 22:1(3)-14:1, and CL 24:1(3)-14:1; linkage location of each PA moiety and *sn* position for fatty acyl chains are not reported. Abundant dianions of all CLs were readily seen, as well as their respective less-abundant monoanions at higher *m/z* values. **Figure 3B** shows the resulting ion/ion reaction from charge inverting all ions from **Figure 3A** with $[Yb(TEHDGA)_3]^{3+}$. The CL dianions, similar to the example shown in **Figure 1B**, formed a positive, singly charged complex via NL of one TEHDGA ligand. Expanding *m/z* 3100-4600 shows low abundance charge inverted CL dianions with all three TEHDGA ligands. Presumably, excess energy from the ion/ion reaction results in the rapid NL of one ligand. CL monoanions are charge inverted to form a positive doubly charged complex around *m/z* 1250-1500 in abundances reflective of their relative abundances of the MS1 in negative ion mode. Similar fragmentation patterns that were observed in **Figure 1C** and **Figure 2** are observed for the CLs here and are shown in **Figures S1** and **S2**. All charge inverted CL dianions first undergo a second NL of one TEHDGA ligand upon CID. A second CID step results in minor NL of each fatty acyl chain as acids, while the most abundant fragment ions reflect phosphodiester cleavages along each PA moiety.

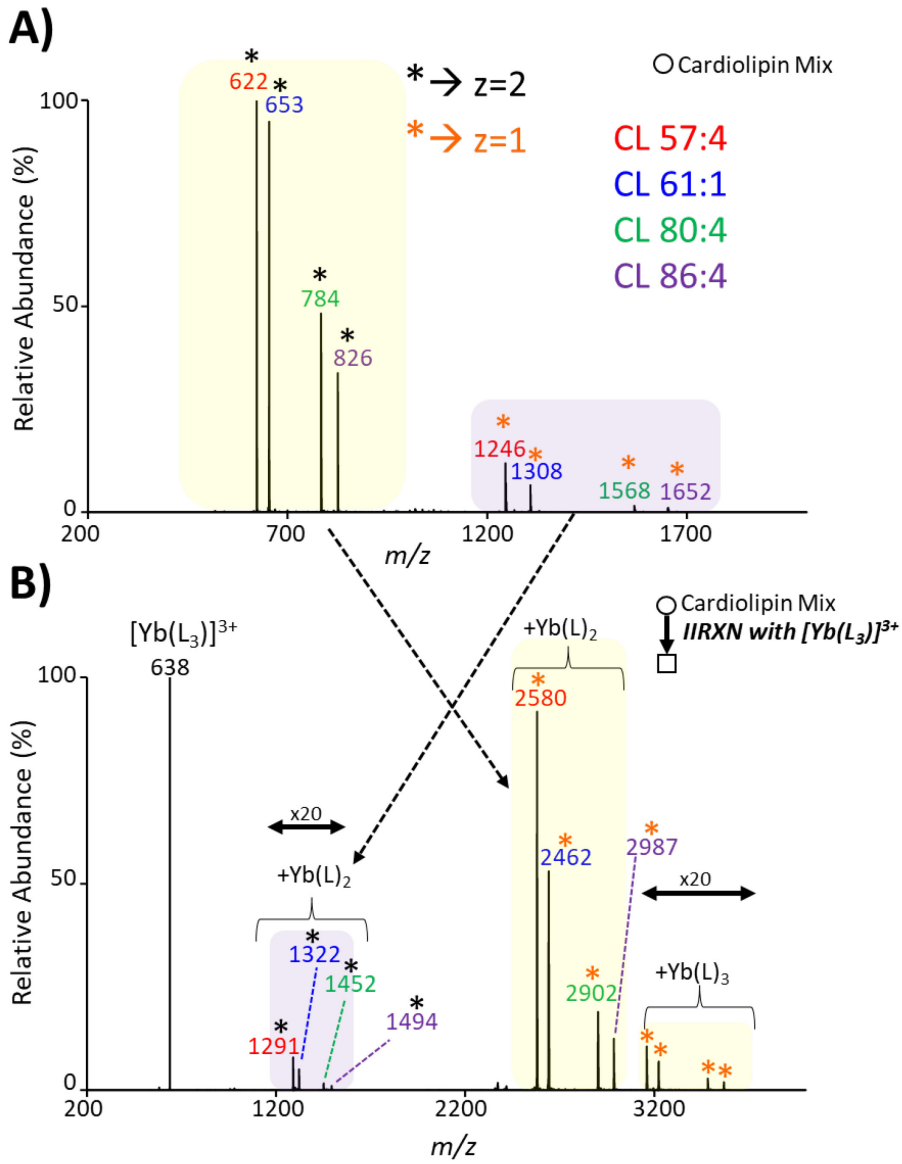

Figure 3. Charge inversion ion/ion reactions between $[Yb(TEHDGA)_3]^{3+}$ and Cardiolipin 1 mix. A) MS1 of negative ion mode nESI of Cardiolipin Mix 1 (CL mix). CL identity is listed as sum fatty acyl composition and color coded. The yellow and purple shaded box indicate similar ion-types and their respective charge is listed in the box. B) Resulting ion/ion reaction from charge inversion of the CL mix. The colored boxes here indicate the precursor ion-type that was charge-inverted. The charge states are once more indicated by a boxed label.

Simultaneous charge inversion of PE and CLs

To further investigate $[Yb(TEHDGA)_3]^{3+}$ as a charge inversion reagent, a preferentially singly charged lipid was utilized, specifically PE 16:0/18:1. As shown in **Figure 3B**, charge inversion of singly charged CLs resulted in a doubly charged complex, which was also observed when using a singly charged PE ion (see **Figure 4A**), though there more products observed for the PE. The base peak from the resulting ion/ion reaction is $[Yb(L_2)+(PE-H)]^{2+}$ (*m/z* 1025.3); there is also a minor ion with all three ligands, $[Yb(L_3)+(PE-H)]^{2+}$ (*m/z* 1315.6). Notably, (*m/z* 2767.2) reflects a second attachment of the PE anion to yield a 1+ complex, $[Yb(L_2)+2(PE-H)]^{+}$, as well as evidence of a NL of an additional ligand at (*m/z*

2186.7). This sequential reaction involves charge inversion to a 2+ complex reacting followed by an additional attachment of a residual PE anion. We note that evidence for the formation of $[Yb(L_2)+2(PE-H)]^+$ was noted even at mutual storage times as low as 1 ms, which suggests that there may have been a small population of doubly-charged PE dimers in the precursor anion population. CID was performed on the second PE attachment in **Figure S3**, where CID of $[[Yb(L_2)+2(PE-H)]^+$ resulted in NL of one ligand (**Figure S3A**) and subsequent CID (**Figure S3B**) revealed fatty acyl chain losses with and without headgroup loss, NL of the last ligand, and phosphodiester cleavage from one of the PE attachments.

Products from sequential attachments of singly-charged anions to the reagent tri-cation (see an example in **Figure 4A**) appear at similar *m/z* ratios to those of the single attachment of a CL di-anion, which can complicate the separation of ions of similar *m/z* but different *z*. A mixture of PE 16:0/18:1 and CL 18:1/18:1 18:1/18:1 was ionized and allowed to react simultaneously with $[Yb(TEHDGA)_3]^{3+}$ to provide the ion/ion reaction product ion spectrum in **Figure 4B.** An abundant charge inverted CL is present, as well as the PE product ions that also appear in **Figure 4A**. For complex mixture analysis, such as identifying low level CLs in the presence of more abundant PEs with similar *m/z*, the resulting ion/ion reaction product identification can be ambiguous. As apparent in **Figure 4A**, the second PE attachment undergoes minor NL of a second TEHDGA, most likely due to excess energy from the ion/ion reaction while the CL product does not. This led to the hypothesis that if both the second PE attachment and CL product shed one ligand during the first CID step (as demonstrated in **Figure 1C**), the PE species may shed it faster than the CL. To explore this possibility, we applied dipolar DC (DDC) collisional activation, a broadband activation technique. We've previously reported various implementations of DDC.[36,52,56,57] It has been demonstrated that changing the applied time of DDC while keeping the voltage constant, pseudo-first order kinetics are observed and thus dissociation rates can be determined. Dissociation rate determination has been able to offer fundamental insights into topics such as gas-phase covalent bond formation energetics,[56,58] determining effective ion temperatures,[57] and lipid isomeric differentiation.[36] Here, we investigated if the PE complex underwent a ligand loss faster than the CL complex by applying DDC first at a constant time of 200 ms and 31 V (**Figure 4C**). With these conditions, only one fragment ion is observed, one ligand loss from the PE complex, with no evidence of the CL complex fragmenting.

To further characterize the apparent difference in kinetic stabilities of the complexes with two PE constituents versus those with a single CL, separate experiments were performed where CL and PE ions were isolated prior to the charge inversion reaction to look at only one product complex at a time. For each precursor ion, the DDC voltage was held at 27 V and the time over which the DDC voltage was applied was varied. The survival yield at each time point was calculated by normalizing all ion abundances and dividing the precursor ion's abundance by the sum of the precursor and all fragments abundance and plotted in **Figure 4D**. At DDC = 27 V, most of the 2nd PE attachment complex was depleted by 550 ms (dissociation rate = 6.3 s^{-1}) whereas no measurable CL complex fragmentation was noted. At DDC = 31 V, a dissociation rate for the CL complex was 0.3 s^{-1}, while that for the complex with two PE constituents was approximately 85.0 s^{-1} (considering only the linear dynamic range), roughly 100x faster (see **Figure S4**). This verified that is it straightforward to establish conditions in which essentially more fragile complexes comprised of two PEs can be dissociated without fragmenting the more stable complexes comprised of a CL.

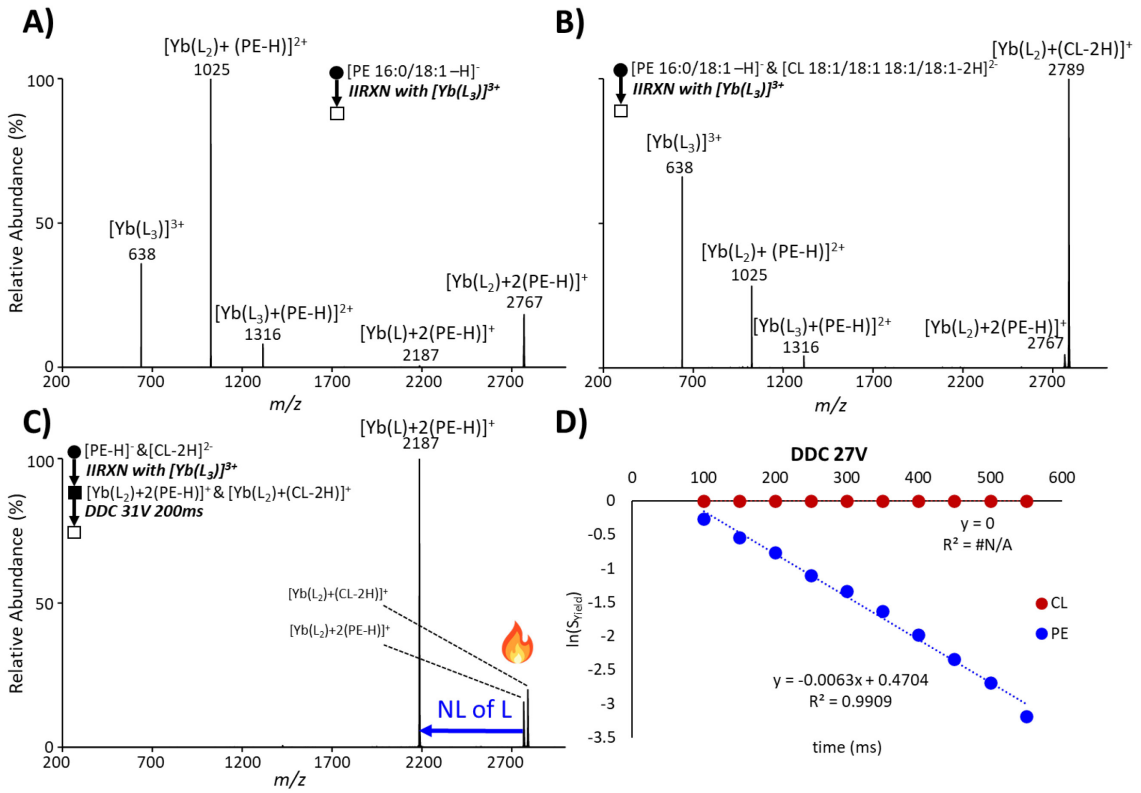

Figure 4. Ion/ion reactions between $[Yb(TEHDGA)_3]^{3+}$ and [PE 16:0/18:1-H]$^-$ and/or [CL 18:1/18:1 18:1/18:1-2H]$^{2-}$ and subsequent activation. A) Ion/ion reaction product ion spectrum of $[Yb(TEHDGA)_3]^{3+}$ and [PE 16:0/18:1-H]$^-$. B) Ion/ion reaction product ion spectrum of $[Yb(TEHDGA)_3]^{3+}$ with a mixture of [PE 16:0/18:1-H]$^-$ and [CL 18:1/18:1 18:1/18:1-2H]$^{2-}$. C) Broadband DDC activation of the charge-inverted PE and CL complexes. D) DDC kinetics of the survival yield for each CL and PE charge inverted complex as a function of time.

Charge inversion of *E. coli* lipid extract

E. coli lipid extract was used as a complex lipid mixture to probe the resulting reaction with $[Yb(TEHDGA)_3]^{3+}$ for chemical charge state separation. **Figure 5A** provides the negative ion-mode MS1 of *E. coli* lipid extract, (*m/z* 700-800), which is presumably a mixture of various singly-charged PE and PGs, as well as doubly-charged CLs. There is a small population of doubly charged ions between (*m/z* 550-610) that is believed to be monolyso-CLs (MLCL), e.g. CLs with one less FA chain. Around (*m/z* 1320-1510) is presumably the singly charged counterparts of the doubly charged CLs, though it may also be a combination of PE and PG dimers. **Figure 5B** reflects the charge inversion ion/ion reaction with all ions from **Figure 5A** with $[Yb(TEHDGA)_3]^{3+}$. Charge inverted PE and PGs with three and two ligands, (~*m/z* 975-1095 and 12565-1385, respectively) are prominent doubly charged species at lower *m/z*. At higher *m/z* (~2660-2940) there is a large distribution of singly charged species that is believed to be a combination of charge inverted CLs and two attachments of PE and/or PGs. In lower abundance but still easily observed, at (~*m/z* 2430-2555) are the putative monolyso-CLs.

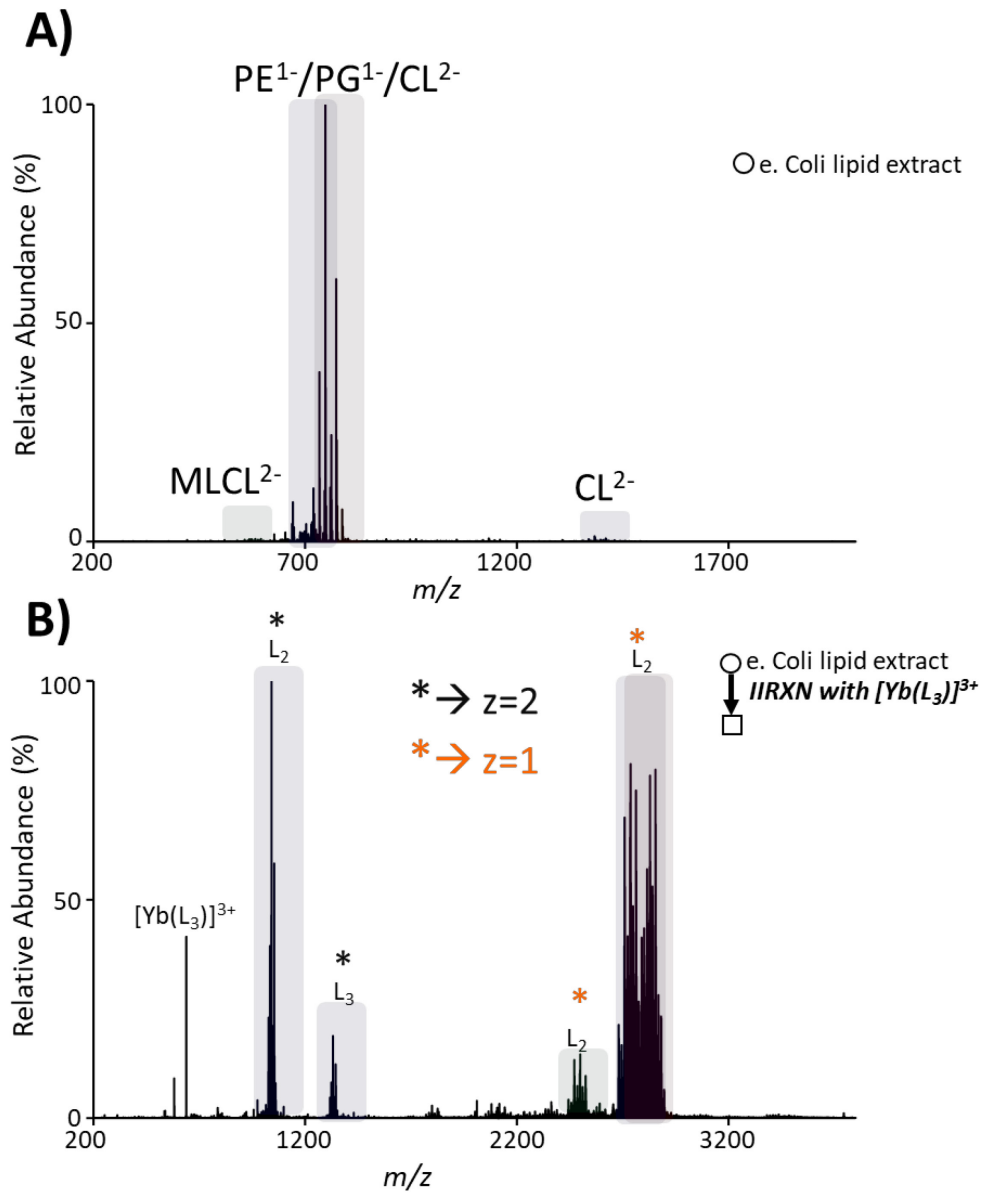

Figure 5. Ion/ion reactions between $[Yb(TEHDGA)_3]^{3+}$ and *E. coli* polar lipid extract. A) Negative ion-mode MS1 of 0.05 mg/mL *E. coli* polar lipid extract. B) Charge inversion product ion spectrum of *E. coli* polar lipid extract reacting with $[Yb(TEHDGA)_3]^{3+}$.

The higher mass ions in **Figure 5B** (*m/z* 2660-2940) are related complexes containing either CLs or two attachments of PE/PG. Taking advantage of the different kinetic stabilities of the CL- and PE/PG-containing species, DDC was used to separate the two ion-types by selectively inducing the loss of one ligand (580.5 Da) from the PE/PG-containing species. This is demonstrated in **Figure 6**, where first the 2nd PE/PG attachment and CL complexes (*m/z* 2660-2940) were isolated via a resonance ejection ramp.[50,59] All four spectra (**Figure 6A-D**) reflect increasing DDC times (A)0, B)50, C)100, and D)200 ms) that show an increasing extent of ligand loss. By 200 ms, essentially all the PE/PG-containing complexes with two ligands are depleted from the isolated population with most being converted to single ligand complexes in the region of (*m/z* 2100-2400). Evidence for a small degree of sequential fragmentation (i.e., from the appearance of ions at m/z 1423-1700) is also apparent and presumed various acyl chain losses from the PE/PG-containing complexes.

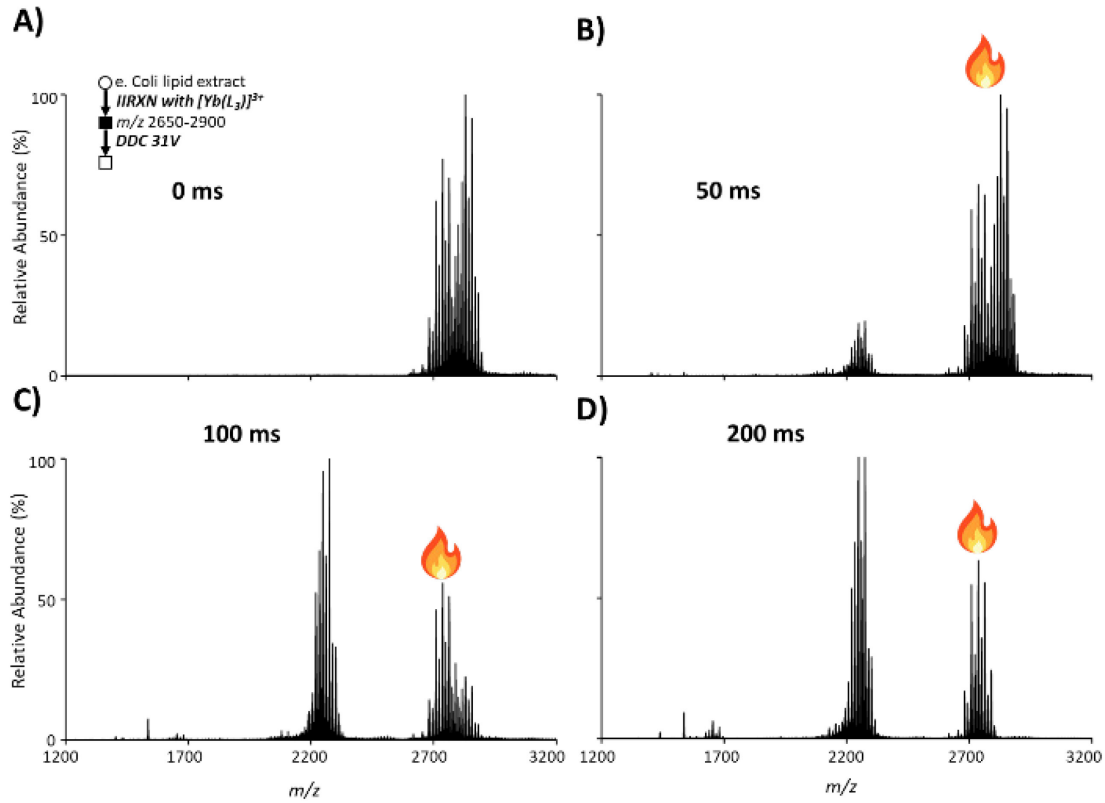

Figure 6. Isolation and subsequent DDC activation of CL-complex and 2(PE/PG)-complex ions post ion/ion reaction of *E. coli* and $[Yb(TEHDGA)_3]^{3+}$. A) Isolation of (*m/z* 2660-2940) following the ion/ion reaction in **Figure 5B**. B) 50 ms of DDC of 31 V of the isolated ion species. C) 100 ms and D) 200 ms of 31 V of the isolated ion species.

A zoom in of no DDC applied, **Figure 7A**, and 200 ms of 31 V of DDC applied, **Figure 7B**, were plotted with their absolute abundance. Comparison of the absolute abundances in Figure 7A and 7B indicates very little ligand loss from the presumed CL-containing ions, as approximately equal abundances of these ions are observed before and after application of the DDC voltage. The PE/PG-containing complexes, on the other hand, are largely depleted. The sum compositions of the CLs found here, some of which are labeled in the expanded region of **Figure 7B**, further enlarged and labeled in **Figure S5**, agree with previous reports of profiling CLs in *E. coli*.[32,60]

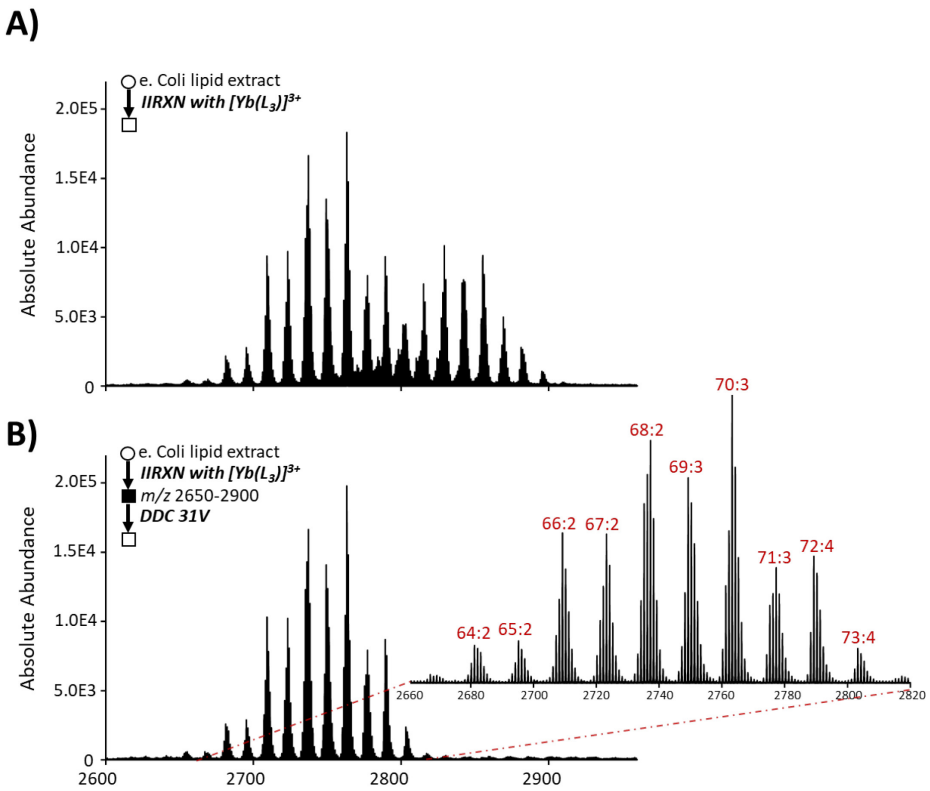

Figure 7. Zoom-in of post-ion/ion reaction of *E. coli* and $[Yb(TEHDGA)_3]^{3+}$ without and with isolation and DDC afterwards. A) Zoom-in of **Figure 5B**, the resulting product ion spectrum. B) Zoom-in of **Figure 6D -**isolation and 31 V applied DDC for 200 ms post ion/ion reaction. The red labels in **B** report CL sum composition.

Conclusions

ESI can give rise to a variety of charge states that can make analysis difficult when differently charged species overlap in *m/z*. Here, a trivalent lanthanide coordinated to three N,N,N',N'-tetra-2-ethylhexyl diglycolamides (TEHDGA) yielded a triply charged cation, $[Yb(TEHDGA)_3]^{3+}$, that was used to charge invert singly- and doubly-charged lipids with similar *m/z*. Charge-inversion of doubly deprotonated CLs yielded a singular product ion, $[Yb(L_2)+(CL-2H)]^+$ (L=TEHDGA), that upon ion-trap CID underwent a NL of one TEHDGA ligand followed by various fatty acyl chain losses upon further CID. Singly-charged PE anions formed a variety of product ions from the ion/ion reaction, i.e $[Yb(L_3)+(PE-H)]^{2+}$,$[Yb(L_2)+(PE-H)]^{2+}$, and more notably second attachment ions $[Yb(L_2)+2(PE-H)]^+$and $[Yb(L)+2(PE-H)]^+$. CID of all latter ions show various degrees of ligand loss as well as fatty acyl chain losses that aid in distinguishing CLs from PEs.

While the second attachment of PE during the ion/ion reaction results in products that are similar in *m/z* to CL product ions, it was found via dissociation kinetics (DDC activation) that the second PE attachment complexes undergo NL of one TEHDGA significantly faster than do CL-containing complexes. The kinetic stabilities of the two types of complexes are sufficiently different that DDC conditions can be established to deplete the PE-containing complexes with little to no loss of the CL-containing complexes. This minimizes spectral congestion while retaining both lipid species for further interrogation via tandem MS. This phenomenon was found to be universal for singly charged PE and PGs and was here demonstrated by subjecting an *E. coli* lipid extract to ion/ion reactions with $[Yb(L_3)]^{3+}$. The overall process involving ion/ion reactions and various CID steps constitutes a 'chemical' means for separating mixtures of singly- and doubly-charged anions that overlap in *m/z*, which is a common situation in the negative nESI of lipid mixtures.

Associated Content

Supporting Information

CID experiments interrogating charge-inverted CL and PE standards, DDC kinetics of charge-inverted *E. coli* anions at 31V, enlarged labeled spectrum of charge-inverted *E. coli* anions after DDC activation.

This material is available free of charge via the Internet at http://pubs.acs.org.

Author Information

Corresponding Author

Scott A. McLuckey – *Department of Chemistry, Purdue University, 560 Oval Drive, West Lafayette, Indiana 47907-2084, United States*

Authors

Kimberly C. Fabijanczuk - *Department of Chemistry, Purdue University, 560 Oval Drive, West Lafayette, Indiana 47907-2084, United States*

David J. Foreman - *Department of Chemistry, Purdue University, 560 Oval Drive, West Lafayette, Indiana 47907-2084, United States*

Author Contributions

K.C.F- conceptualization, methodology, visualization, writing-original draft; D.J.F- conceptualization, writing-review and editing; S.A.M- conceptualization, writing-review and editing, supervision, project administration.

Conflicts of Interest

The authors declare no competing financial interest.

Acknowledgments

This work was funded and supported by the National Science Foundation CHE-2304386 and Sciex. We thank Dr. Christopher A. Zarzana and Dr. Brittany D. Hodges for their introduction and protocol preparation for N,N,N',N'-tetra-2-ethylhexyl diglycolamide (TEHDGA).

References

(1) Fenn, J. B.; Mann, M.; Meng, C. K.; Wong, S. F.; Whitehouse, C. M. Electrospray Ionization for Mass Spectrometry of Large Biomolecules. *Science (1979)* **1989**, *246* (4926), 64–71. https://doi.org/10.1126/science.2675315.

(2) Smith, R. D.; Loo, J. A.; Edmonds, C. G.; Barinaga, C. J.; Udseth, H. R. New Developments in Biochemical Mass Spectrometry: Electrospray Ionization. *Anal Chem* **1990**, *62* (9), 882–899. https://doi.org/10.1021/ac00208a002.

(3) Kim, H.-Yong.; Wang, T.-C. L.; Ma, Y.-Chung. Liquid Chromatography/Mass Spectrometry of Phospholipids Using Electrospray Ionization. *Anal Chem* **1994**, *66* (22), 3977–3982. https://doi.org/10.1021/ac00094a020.

(4) Fenn, J. B. Electrospray Wings for Molecular Elephants (Nobel Lecture). In *Angewandte Chemie - International Edition*; 2003; Vol. 42, pp 3871–3894. https://doi.org/10.1002/anie.200300605.

(5) Konermann, L.; Ahadi, E.; Rodriguez, A. D.; Vahidi, S. Unraveling the Mechanism of Electrospray Ionization. *Anal Chem* **2013**, *85* (1), 2–9. https://doi.org/10.1021/ac302789c.

(6) Wang, G.; Cole, R. Solution, Gas-Phase, and Instrumental Parameter Influences on Charge-State Distributions in Electrospray Ionization Mass Spectrometry. In *Electrospray ionization mass spectrometry*; Wiley: New York, 1997; pp 137–174.

(7) Zhou, S.; Cook, K. D. A Mechanistic Study of Electrospray Mass Spectrometry: Charge Gradients within Electrospray Droplets and Their Influence on Ion Response. *J Am Soc Mass Spectrom* **2001**, *12* (2), 206–214. https://doi.org/10.1016/S1044-0305(00)00213-0.

(8) Tang, Liang.; Kebarle, Paul. Dependence of Ion Intensity in Electrospray Mass Spectrometry on the Concentration of the Analytes in the Electrosprayed Solution. *Anal Chem* **1993**, *65* (24), 3654–3668. https://doi.org/10.1021/ac00072a020.

(9) Flick, T. G.; Cassou, C. A.; Chang, T. M.; Williams, E. R. Solution Additives That Desalt Protein Ions in Native Mass Spectrometry. *Anal Chem* **2012**, *84* (17), 7511–7517. https://doi.org/10.1021/ac301629s.

(10) Hale, O. J.; Cramer, R. Collision-Induced Dissociation of Doubly-Charged Barium-Cationized Lipids Generated from Liquid Samples by Atmospheric Pressure Matrix-Assisted Laser Desorption/Ionization Provides Structurally Diagnostic Product Ions. *Anal Bioanal Chem* **2018**, *410* (5), 1435–1444. https://doi.org/10.1007/s00216-017-0788-6.

(11) Geue, N.; Bennett, T. S.; Ramakers, L. A. I.; Timco, G. A.; McInnes, E. J. L.; Burton, N. A.; Armentrout, P. B.; Winpenny, R. E. P.; Barran, P. E. Adduct Ions as Diagnostic Probes of Metallosupramolecular Complexes Using Ion Mobility Mass Spectrometry. *Inorg Chem* **2023**, *62* (6), 2672–2679. https://doi.org/10.1021/acs.inorgchem.2c03698.

(12) Sasiene, Z. J.; Ropartz, D.; Rogniaux, H.; Jackson, G. P. Charge Transfer Dissociation of a Branched Glycan with Alkali and Alkaline Earth Metal Adducts. *Journal of Mass Spectrometry* **2021**, *56* (7). https://doi.org/10.1002/jms.4774.

(13) King, R.; Bonfiglio, R.; Fernandez-Metzler, C.; Miller-Stein, C.; Olah, T. Mechanistic Investigation of Ionization Suppression in Electrospray Ionization. *J Am Soc Mass Spectrom* **2000**, *11* (11), 942–950. https://doi.org/10.1016/S1044-0305(00)00163-X.

(14) Leney, A. C.; Heck, A. J. R. Native Mass Spectrometry: What Is in the Name? *J Am Soc Mass Spectrom* **2017**, *28* (1), 5–13. https://doi.org/10.1007/s13361-016-1545-3.

(15) Herron, W. J.; Goeringer, D. E.; McLuckey, S. A. Product Ion Charge State Determination via Ion/Ion Proton Transfer Reactions. *Anal Chem* **1996**, *68* (2), 257–262. https://doi.org/10.1021/ac950895b.

(16) Stephenson, J. L.; McLuckey, S. A. Simplification of Product Ion Spectra Derived from Multiply Charged Parent Ions via Ion/Ion Chemistry. *Anal Chem* **1998**, *70* (17), 3533–3544. https://doi.org/10.1021/ac9802832.

(17) Coon, J. J.; Ueberheide, B.; Syka, J. E. P.; Dryhurst, D. D.; Ausio, J.; Shabanowitz, J.; Hunt, D. F. Protein Identification Using Sequential Ion/Ion Reactions and Tandem Mass Spectrometry. *Proceedings of the National Academy of Sciences* **2005**, *102* (27), 9463–9468. https://doi.org/10.1073/pnas.0503189102.

(18) McLuckey, S. A.; Huang, T.-Y. Ion/Ion Reactions: New Chemistry for Analytical MS. *Anal Chem* **2009**, *81* (21), 8669–8676. https://doi.org/10.1021/ac9014935.

(19) Stephenson, J. L.; McLuckey, S. A. Ion/Ion Reactions in the Gas Phase: Proton Transfer Reactions Involving Multiply-Charged Proteins. *J Am Chem Soc* **1996**, *118* (31), 7390–7397. https://doi.org/10.1021/ja9611755.

(20) Liang, X.; McLuckey, S. A. Transmission Mode Ion/Ion Proton Transfer Reactions in a Linear Ion Trap. *J Am Soc Mass Spectrom* **2007**, *18* (5), 882–890. https://doi.org/10.1016/j.jasms.2007.02.001.

(21) Ugrin, S. A.; English, A. M.; Syka, J. E. P.; Bai, D. L.; Anderson, L. C.; Shabanowitz, J.; Hunt, D. F. Ion-Ion Proton Transfer and Parallel Ion Parking for the Analysis of Mixtures of Intact Proteins on a Modified Orbitrap Mass Analyzer. *J Am Soc Mass Spectrom* **2019**, *30* (10), 2163–2173. https://doi.org/10.1007/s13361-019-02290-8.

(22) Newton, K. A.; Amunugama, R.; McLuckey, S. A. Gas-Phase Ion/Ion Reactions of Multiply Protonated Polypeptides with Metal Containing Anions. *J Phys Chem A* **2005**, *109* (16), 3608–3616. https://doi.org/10.1021/jp044106i.

(23) Gunawardena, H. P.; O'Hair, R. A. J.; McLuckey, S. A. Selective Disulfide Bond Cleavage in Gold(I) Cationized Polypeptide Ions Formed via Gas-Phase Ion/Ion Cation Switching. *J Proteome Res* **2006**, *5* (9), 2087–2092. https://doi.org/10.1021/pr0602794.

(24) Crizer, D. M.; Xia, Y.; McLuckey, S. A. Transition Metal Complex Cations as Reagents for Gas-Phase Transformation of Multiply Deprotonated Polypeptides. *J Am Soc Mass Spectrom* **2009**, *20* (9), 1718–1722. https://doi.org/10.1016/j.jasms.2009.05.008.

(25) Han, H.; McLuckey, S. A. Selective Covalent Bond Formation in Polypeptide Ions via Gas-Phase Ion/Ion Reaction Chemistry. *J Am Chem Soc* **2009**, *131* (36), 12884–12885. https://doi.org/10.1021/ja904812d.

(26) McGee, W. M.; Mentinova, M.; McLuckey, S. A. Gas-Phase Conjugation to Arginine Residues in Polypeptide Ions via *N* -Hydroxysuccinimide Ester-Based Reagent Ions. *J Am Chem Soc* **2012**, *134* (28), 11412–11414. https://doi.org/10.1021/ja304778j.

(27) Peng, Z.; Pilo, A. L.; Luongo, C. A.; McLuckey, S. A. Gas-Phase Amidation of Carboxylic Acids with Woodward's Reagent K Ions. *J Am Soc Mass Spectrom* **2015**, *26* (10), 1686–1694. https://doi.org/10.1007/s13361-015-1209-8.

(28) Bu, J.; Fisher, C. M.; Gilbert, J. D.; Prentice, B. M.; McLuckey, S. A. Selective Covalent Chemistry via Gas-Phase Ion/Ion Reactions: An Exploration of the Energy Surfaces Associated with N-Hydroxysuccinimide Ester Reagents and Primary Amines and Guanidine Groups. *J Am Soc Mass Spectrom* **2016**, *27* (6), 1089–1098. https://doi.org/10.1007/s13361-016-1359-3.

(29) Carvalho, V. V.; See Kit, M. C.; Webb, I. K. Ion Mobility and Gas-Phase Covalent Labeling Study of the Structure and Reactivity of Gaseous Ubiquitin Ions Electrosprayed from Aqueous and Denaturing Solutions. *J Am Soc Mass Spectrom* **2020**, *31* (5), 1037–1046. https://doi.org/10.1021/jasms.9b00138.

(30) Randolph, C. E.; Foreman, D. J.; Betancourt, S. K.; Blanksby, S. J.; McLuckey, S. A. Gas-Phase Ion/Ion Reactions Involving Tris-Phenanthroline Alkaline Earth Metal Complexes as Charge Inversion Reagents for the Identification of Fatty Acids. *Anal Chem* **2018**, *90* (21), 12861–12869. https://doi.org/10.1021/acs.analchem.8b03441.

(31) Randolph, C. E.; Marshall, D. L.; Blanksby, S. J.; McLuckey, S. A. Charge-Switch Derivatization of Fatty Acid Esters of Hydroxy Fatty Acids via Gas-Phase Ion/Ion Reactions. *Anal Chim Acta* **2020**, *1129*, 31–39. https://doi.org/10.1016/j.aca.2020.07.005.

(32) Randolph, C. E.; Fabijanczuk, K. C.; Blanksby, S. J.; McLuckey, S. A. Proton Transfer Reactions for the Gas-Phase Separation, Concentration, and Identification of Cardiolipins. *Anal Chem* **2020**, *92* (15), 10847–10855. https://doi.org/10.1021/acs.analchem.0c02545.

(33) Randolph, C. E.; Shenault, D. M.; Blanksby, S. J.; McLuckey, S. A. Localization of Carbon–Carbon Double Bond and Cyclopropane Sites in Cardiolipins via Gas-Phase Charge Inversion Reactions. *J Am Soc Mass Spectrom* **2021**, *32* (2), 455–464. https://doi.org/10.1021/jasms.0c00348.

(34) Chao, H.-C.; McLuckey, S. A. In-Depth Structural Characterization and Quantification of Cerebrosides and Glycosphingosines with Gas-Phase Ion Chemistry. *Anal Chem* **2021**, *93* (19). https://doi.org/10.1021/acs.analchem.1c01021.

(35) Chao, H.-C.; McLuckey, S. A. Manipulation of Ion Types via Gas-Phase Ion/Ion Chemistry for the Structural Characterization of the Glycan Moiety on Gangliosides. *Anal Chem* **2021**, *93* (47), 15752–15760. https://doi.org/10.1021/acs.analchem.1c03876.

(36) Fabijanczuk, K. C.; Chao, H.-C.; Fischer, J. L.; McLuckey, S. A. Structural Elucidation and Isomeric Differentiation/Quantitation of Monophosphorylated Phosphoinositides Using Gas-Phase Ion/Ion Reactions and Dissociation Kinetics. *Analyst* **2022**. https://doi.org/10.1039/D2AN00792D.

(37) Randolph, C. E.; Beveridge, C. H.; Iyer, S.; Blanksby, S. J.; McLuckey, S. A.; Chopra, G. Identification of Monomethyl Branched-Chain Lipids by a Combination of Liquid Chromatography Tandem Mass Spectrometry and Charge-Switching Chemistries. *J Am Soc Mass Spectrom* **2022**. https://doi.org/10.1021/jasms.2c00225.

(38) Madalinski, G.; Fournier, F.; Wind, F.-L.; Afonso, C.; Tabet, J.-C. Gram-Negative Bacterial Lipid A Analysis by Negative Electrospray Ion Trap Mass Spectrometry: Stepwise Dissociations of Deprotonated Species under Low Energy CID Conditions. *Int J Mass Spectrom* **2006**, *249–250*, 77–92. https://doi.org/10.1016/j.ijms.2005.12.049.

(39) Han, X.; Yang, K.; Yang, J.; Cheng, H.; Gross, R. W. Shotgun Lipidomics of Cardiolipin Molecular Species in Lipid Extracts of Biological Samples. *J Lipid Res* **2006**, *47* (4), 864–879. https://doi.org/10.1194/jlr.D500044-JLR200.

(40) Michelsen, P.; Jergil, B.; Odham, G. *Quantification of Polyphosphoinositides Using Selected Ion Monitoring Electrospray Mass Spectrometry*; 1995; Vol. 9.

(41) Pettitt, T. R.; Dove, S. K.; Lubben, A.; Calaminus, S. D. J.; Wakelam, M. J. O. Analysis of Intact Phosphoinositides in Biological Samples. *J Lipid Res* **2006**, *47* (7), 1588–1596. https://doi.org/10.1194/jlr.D600004-JLR200.

(42) Blanksby, S. J.; Mitchell, T. W. Advances in Mass Spectrometry for Lipidomics. *Annual Review of Analytical Chemistry* **2010**, *3* (1), 433–465. https://doi.org/10.1146/annurev.anchem.111808.073705.

(43) Holčapek, M.; Liebisch, G.; Ekroos, K. Lipidomic Analysis. *Anal Chem* **2018**, *90* (7), 4249–4257. https://doi.org/10.1021/acs.analchem.7b05395.

(44) Züllig, T.; Köfeler, H. C. HIGH RESOLUTION MASS SPECTROMETRY IN LIPIDOMICS. *Mass Spectrom Rev* **2021**, *40* (3), 162–176. https://doi.org/10.1002/mas.21627.

(45) Hsu, F.-F. Mass Spectrometry-Based Shotgun Lipidomics – a Critical Review from the Technical Point of View. *Anal Bioanal Chem* **2018**, *410* (25), 6387–6409. https://doi.org/10.1007/s00216-018-1252-y.

(46) Han, X.; Gross, R. W. Shotgun Lipidomics: Electrospray Ionization Mass Spectrometric Analysis and Quantitation of Cellular Lipidomes Directly from Crude Extracts of Biological Samples. *Mass Spectrom Rev* **2005**, *24* (3), 367–412. https://doi.org/10.1002/mas.20023.

(47) Gross, R. W.; Han, X. Lipidomics at the Interface of Structure and Function in Systems Biology. *Chem Biol* **2011**, *18* (3), 284–291. https://doi.org/10.1016/j.chembiol.2011.01.014.

(48) Zhang, W.; Jian, R.; Zhao, J.; Liu, Y.; Xia, Y. Deep-Lipidotyping by Mass Spectrometry: Recent Technical Advances and Applications. *J Lipid Res* **2022**, *63* (7), 100219. https://doi.org/10.1016/j.jlr.2022.100219.

(49) Fabijanczuk, K. C.; Hager, J. W.; McLuckey, S. A. Separation and Simultaneous Trapping of Multiply Charged and Singly Charged Ions for Mass Spectrometry:

Application to Lipid Mixtures. *Anal Chem* **2023**, *95* (14), 6115–6121. https://doi.org/10.1021/acs.analchem.3c00420.

(50) Bhanot, J. S.; Fabijanczuk, K. C.; Abdillahi, A. M.; Chao, H.-C.; Pizzala, N. J.; Londry, F. A.; Dziekonski, E. T.; Hager, J. W.; McLuckey, S. A. Adaptation and Operation of a Quadrupole/Time-of-Flight Tandem Mass Spectrometer for High Mass Ion/Ion Reaction Studies. *Int J Mass Spectrom* **2022**, *478*, 116874. https://doi.org/10.1016/j.ijms.2022.116874.

(51) Xia, Y.; Liang, X.; McLuckey, S. A. Pulsed Dual Electrospray Ionization for Ion/Ion Reactions. *J Am Soc Mass Spectrom* **2005**, *16* (11), 1750–1756. https://doi.org/10.1016/j.jasms.2005.07.013.

(52) Webb, I. K.; Londry, F. A.; McLuckey, S. A. Implementation of Dipolar Direct Current (DDC) Collision-Induced Dissociation in Storage and Transmission Modes on a Quadrupole/Time-of-Flight Tandem Mass Spectrometer. *Rapid Communications in Mass Spectrometry* **2011**, *25* (17). https://doi.org/10.1002/rcm.5152.

(53) Ansari, S. A.; Pathak, P.; Mohapatra, P. K.; Manchanda, V. K. Chemistry of Diglycolamides: Promising Extractants for Actinide Partitioning. *Chem Rev* **2012**, *112* (3), 1751–1772. https://doi.org/10.1021/cr200002f.

(54) Gong, Y.; Tian, G.; Rao, L.; Gibson, J. K. Dissociation of Diglycolamide Complexes of Ln^{3+} (Ln = La–Lu) and An^{3+} (An = Pu, Am, Cm): Redox Chemistry of 4f and 5f Elements in the Gas Phase Parallels Solution Behavior. *Inorg Chem* **2014**, *53* (22), 12135–12140. https://doi.org/10.1021/ic501985p.

(55) Hsu, F.-F.; Turk, J.; Rhoades, E. R.; Russell, D. G.; Shi, Y.; Groisman, E. A. Structural Characterization of Cardiolipin by Tandem Quadrupole and Multiple-Stage Quadrupole Ion-Trap Mass Spectrometry with Electrospray Ionization. *J Am Soc Mass Spectrom* **2005**, *16* (4), 491–504. https://doi.org/10.1016/j.jasms.2004.12.015.

(56) Bu, J.; Fisher, C. M.; Gilbert, J. D.; Prentice, B. M.; McLuckey, S. A. Selective Covalent Chemistry via Gas-Phase Ion/Ion Reactions: An Exploration of the Energy Surfaces Associated with N-Hydroxysuccinimide Ester Reagents and Primary Amines and Guanidine Groups. *J Am Soc Mass Spectrom* **2016**, *27* (6), 1089–1098. https://doi.org/10.1007/s13361-016-1359-3.

(57) Mehnert, S. A.; Fischer, J. L.; McDaniel, M. R.; Fabijanczuk, K. C.; McLuckey, S. A. Dissociation Kinetics in Quadrupole Ion Traps: Effective Temperatures under Dipolar DC Collisional Activation Conditions. *J Am Soc Mass Spectrom* **2023**.

(58) Fischer, J. L.; Mehnert, S. A.; Pitts-McCoy, A. M.; McLuckey, S. A. Gas-Phase Covalent Bond Formation via Nucleophilic Substitution: A Dissociation Kinetics Study of Leaving Groups, Isomeric R Groups, and Nucleophilic Sites. *J Am Soc Mass Spectrom* **2022**, *33* (8), 1346–1354. https://doi.org/10.1021/jasms.2c00003.

(59) McLuckey, S. A.; Goeringer, D. E.; Glish, G. L. Selective Ion Isolation/Rejection over a Broad Mass Range in the Quadrupole Ion Trap. *J Am Soc Mass Spectrom* **1991**, *2* (1), 11–21. https://doi.org/10.1016/1044-0305(91)80056-D.

(60) Macias, L. A.; Feider, C. L.; Eberlin, L. S.; Brodbelt, J. S. Hybrid 193 Nm Ultraviolet Photodissociation Mass Spectrometry Localizes Cardiolipin Unsaturations. *Anal Chem* **2019**, *91* (19), 12509–12516. https://doi.org/10.1021/acs.analchem.9b03278.

TOC